Proceedings of the ASME 2020 International Design Engineering Technical Conferences & Computers and Information in Engineering Conference
IDETC/CIE 2020
August 16-19, 2020, St. Louis, MO, USA

BI-LEVEL OPTIMIZATION FOR ELECTRICITY TRANSACTION IN SMART COMMUNITY WITH MODULAR PUMP HYDRO STORAGE

Yang Chen*
Environmental Sciences Division
Oak Ridge National Laboratory
Oak Ridge, U.S.

Xiao Kou
Department of Electrical
Engineering and Computer Science
University of Tennessee, Knoxville, U.S.

Mohammed Olama, Helia Zandi
Computational Sciences and Engineering
Division, Oak Ridge National Laboratory
Oak Ridge, U.S.

Chenang Liu
School of Industrial
Engineering & Management
Oklahoma State University, Stillwater, U.S.

Saiid Kassaee
Department of Mechanical,
Aerospace, and Biomedical Engineering
University of Tennessee, Knoxville, U.S.

Brennan T. Smith
Environmental Sciences Division
Oak Ridge National Laboratory
Oak Ridge, U.S.

Ahmad Abu-Heiba, Ayyoub M. Momen
Energy and Transportation Science Division
Oak Ridge National Laboratory
Oak Ridge, U.S.

ABSTRACT

Grid integration of the increasing distributed energy resources could be challenging in terms of new infrastructure investment, power grid stability, etc. To resolve more renewables locally and reduce the need for extensive electricity transmission, a community energy transaction market is assumed with market operator as the leader whose responsibility is to generate local energy prices and clear the energy transaction payment among the prosumers (followers). The leader and multi-followers have competitive objectives of revenue maximization and operational cost minimization. This non-cooperative leader-follower (Stackelberg) game is formulated using a bi-level optimization framework, where a novel modular pump hydro storage technology (GLIDES system) is set as an upper level market operator, and the lower level prosumers are nearby commercial buildings. The best responses of the lower level model could be derived by necessary optimality conditions, and thus the bi-level model could be transformed into single level optimization model via replac-

*Corresponding Email: cheny2@ornl.gov. This manuscript has been authored in part by UT-Battelle, LLC, under contract DE-AC05-00OR22725 with the US Department of Energy (DOE). The US government retains and the publisher, by accepting the article for publication, acknowledges that the US government retains a nonexclusive, paid-up, irrevocable, worldwide license to publish or reproduce the published form of this manuscript, or allow others to do so, for US government purposes. DOE will provide public access to these results of federally sponsored research in accordance with the DOE Public Access Plan (http://energy.gov/downloads/doe-public-access-plan).

ing the lower level model by its Karush-Kuhn-Tucker (KKT) necessary conditions. Several experiments have been designed to compare the local energy transaction behavior and profit distribution with the different demand response levels and different local price structures. The experimental results indicate that the lower level prosumers could benefit the most when local buying and selling prices are equal, while maximum revenue potential for the upper level agent could be reached with non-equal trading prices.

1 INTRODUCTION

Aiming at reducing carbon dioxide emissions and slowing down temperature increase under the Paris Agreement, clean electricity underpins almost all efforts to shift towards decarbonisation worldwide. Based on Renewables 2019 Global Status Report [1], a total of 181 gigawatts of renewable power was added in year 2018, and the global renewable power capacity reached 2,378 gigawatts. For the fourth year in a row, additions of renewable power generation capacity outpaced net installations of fossil fuel and nuclear power combined. In the U.S., renewable energy sources accounted for about 11% of the total U.S. energy consumption and about 17% of the electricity generation in year 2018. In the latest long-term projections, the U.S. Energy Information Administration projects electricity generation from renewable sources such as wind and solar to surpass nuclear and coal by year 2021 and to surpass natural gas in year 2045 [2].

Due to the intermittent nature of renewables, efficient energy storage is critical in aiding the integration of variable renewable generation and supporting for more resilient power grids by providing a portfolio of grid services, such as peak demand shaving/reduction, system balancing services (fast frequency response, contingency reserves), transmission services (congestion relief, etc.) [3] [4]. Although various energy storage technologies are in developing phases, four storage types are considered deployed: Pumped Hydroelectric Storage (PHS), Compressed Air Energy Storage (CAES), Advanced Battery Energy Storage (ABES), and Flywheel Energy Storage (FES) [5]. PHS and CAES are large-scale technologies capable of discharge times of tens of hours and capacities up to 1GW. ABES and FES have lower power and shorter discharge times (from seconds to 6 hours) with a very high cost. The first U.S. grid scale energy storage facility was the Rocky River Pumped Storage plant in 1929 on Housatonic River, Connecticut [6], and the largest pumped hydro facility in the world is in Bath County, VA, U.S. with a capacity of 3GW [7]. However, PHS and CAES are geographically limited and there are very limited locations remaining. To address the need for a more ideal energy storage, Ground-Level Integrated Diverse Energy Storage (GLIDES) was invented aiming at favorable characters of high efficiency, low capital cost, and scalability without geographic constraints. GLIDES is modular pump hydro storage technology, it could be treated as the combination of compressed air energy storage (CAES) and conventional PHS [8], details on the main difference and system configuration will be explained in the next section. Most recently, in year 2020, the U.S. Department of Energy has launched the Energy Storage Grand Challenge program to accelerate the development, commercialization, and utilization of the next-generation energy storage technologies.

The arising renewables and storage technologies have attracted more and more attentions on the potential from demand side management instead of traditional generation dominant operations in the grid. Under that context, the traditional energy consumer (e.g. building) has been transformed into a prosumer (producer & consumer) that could interact with the power grid via two-way communication capability, where storage systems enable the flexibility for demand response. For instance, several studies have presented the estimation framework to quantify demand response potential for aggregated residential and commercial buildings [9] [10]. Also a lot of different pricing strategies for utility companies have been proposed to better leverage response potential using a Stackelberg game [11] [12] [13] and data-driven approaches [14]. Besides the research efforts of incentivizing the demand side to participate in market services at the transmission level or distribution level, local energy transactions at the community level [15] are also motivated by the decentralized local renewable generation and the noticeable power loss in distribution networks. Fair profit distribution via business model ensures the creation and operation of such a market. Several models have been proposed to guarantee the relative and absolute fairness in balancing collective and individual interests [16], and the results demonstrate the existence of optimal local transaction price that could maximize the absolute benefit for each participants in the clusters. Different architectures have been proposed for local transaction, for example, peer-to-peer energy trading topology [17], and bi-level energy transaction framework [18] [19]. Some previous works on bi-level energy trading are: one hour price determination of a retailer in the wholesale market and the consumption scheduling of flexible consumers [20], and one hour simultaneous operation of distribution companies and microgrids [21]. The most related work to this study is in [22], where a retailer with storage decides internal sharing prices at the upper level and prosumer microgrids response to the prices by deciding their energy sharing profiles. All related works presume that the internal buying price is greater than the selling price which is generally true at the utility or retailer level, however, at the community level, as independent building prosumers, they will compare their gains with a separate operation and may prefer equal price structure for more fair negotiation. With the consideration of the high battery degradation cost and return-of-investment advantage of GLIDES over battery storage at large scale [8], we adopt the GLIDES system at the upper level for potential large-scale applications.

In this research, the energy trading problem at a commu-

nity level is modeled as non-cooperative leader-follower game with competitive objectives. Correspondingly, a general bi-level optimization model is developed with the local market operator (with GLIDES) as a leader and the prosumers as participants. In designed experiments, different local price structures have been proposed to compare the profit distribution. This paper is organized as follows: Section 2 provides a brief description on the invented modular pump hydro storage technology. Section 3 models the local energy trading problem in a bi-level optimization framework. Section 4 presents the experimental results. And conclusions are drawn in Section 5.

2 GLIDES System Description

As descried in invention patent [23], a typical GLIDES system consists of a liquid storage reservoir, pre-pressurized pressure vessel(s), a pump/motor, and a hydraulic turbine/generator, see Figure 1. The electricity is stored by using pump/motor to pump liquid (e.g. water, oil, etc.) into the pressure vessel with pre-pressurized gas (e.g. air, carbon dioxide, etc.). In discharging process, the now high-head water will be pushed by high pressure gas through the hydraulic turbine to drive the electricity generator. More details on the GLIDES system and its thermal dynamics can be found in our previous studies [4] [24] [25].

As a modular pump hydro storage, the main difference between GLIDES and CAES is that it uses generally a high efficient hydraulic machinery (water pump/turbine) instead of a gas compressor/turbine. Also, it uses compressed air pressure to create a high water head instead of lifting the water body to a upper reservoir (usually the mountain top). This design has eliminated the geographical location limitation of conventional PHS (needs water reservoir) and underground CAES (needs underground cavern). In summary, the GLIDES system has several advantages: 1) it can be installed at ground level or below, basically anywhere that can structurally support the pressure vessels; 2) it has the ability to integrate a diverse range of low grade heat sources and use the waste heat to boost efficiency in the discharging process; 3) it is scalable which makes it possible to be allocated and utilized at the grid-scale or equipped for smart buildings for behind-meter applications (see modular version in Figure 2-3). Storage technologies with similar advantages could be found in liquid air energy storage [26] and pumped thermal electricity storage [27].

The first-generation of the GLIDES prototype (see Figure 4) has been designed to operate between 70-130 bar pressure range with four 500 L vessels. In accounting for pump/motor, turbine and electric generator losses, the 91% indicated efficiency reduces to 66% round-trip efficiency for the first-generation of GLIDES. For second generation of GLIDES, 84% round-trip efficiency could be achieved. Please note that the round-trip efficiency greatly depends on different configurations and turbomachinery efficiencies [24] [25], and about 80% of the capital cost is on the pressure vessel. Several cost reduction opportunities of the GLIDES system is explored in [28].

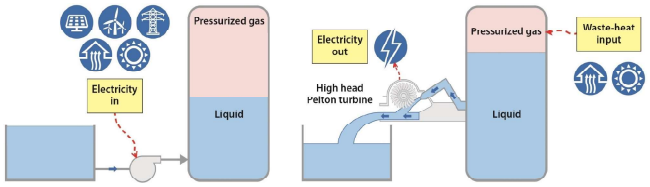

(a) Charging (b) Discharging

FIGURE 1: Basic layout and components of GLIDES system

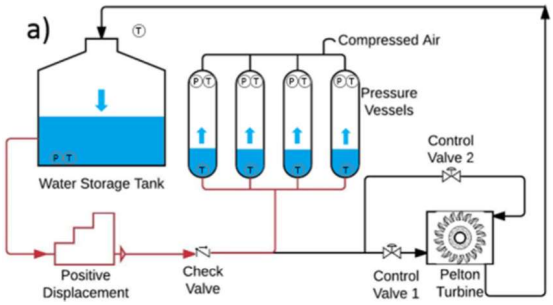

FIGURE 2: Charging process for modular GLIDES prototype schematic

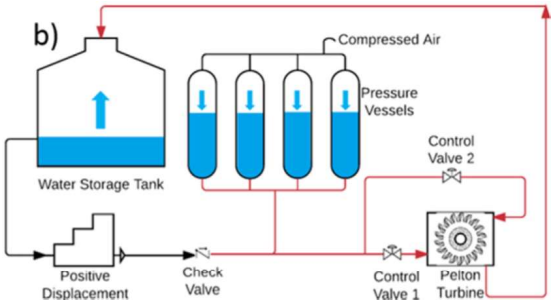

FIGURE 3: Discharging process for modular GLIDES prototype schematic

3 Bi-level Optimization Model

In the bi-level optimization here, the local market operator at the upper level owns the GLIDES system, and the lower level

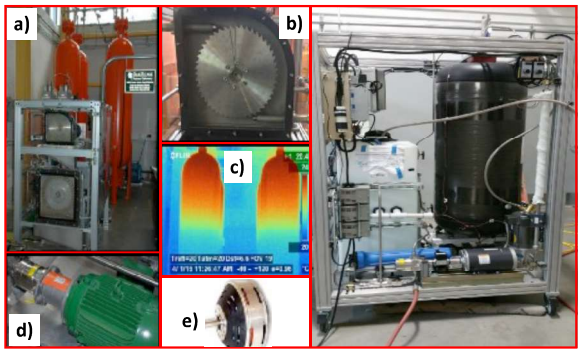

FIGURE 4: Prototypes of first (left) and second (right) generation GLIDES. a) pressure vessels, b) pelton turbine, c) IR image in charging, d) charging pump/motor, e) electric generator

prosumers are equipped with solar photovoltaic (PV) panels and battery storage. The lower level prosumers don't have direct connection with the external power grid and can only buy/sell energy from/to local energy market. The surplus or unsatisfied energy demand in the local market will be transacted with the external power grid through the upper level market operator.

3.1 Upper level model

1) Objective function for local market

$$\begin{aligned}\max OR = \sum_t [&(Ps_t \cdot es_t - Pp_t \cdot ep_t) \\ &+ (pt_t^+ \cdot \sum_n et_{n,t}^i - pt_t^- \cdot \sum_n et_{n,t}^o)]\end{aligned} \tag{1}$$

The objective of the local market operator at the upper level is to maximize its own revenue OR, including revenue in the transaction process with the external power grid (first term in Eq.(1)) and the revenue from the local transaction market (second term in Eq.(1)). $et_{n,t}^i$ and $et_{n,t}^o$ are local energy transaction amount, defined in Table 2. Different from the battery storage at the lower level, the degradation cost of GLIDES can be neglected.

2) Price range in local market

$$Ps_t \le pt_t^- \le pt_t^+ \le Pp_t \tag{2}$$

To absorb more distributed renewables locally and encourage prosumers to participate into the local energy transaction market, the transaction (purchasing and selling) prices are set to be within external price range in Eq.(2).

3) Load balance in local market

$$ep_t + eg_t + \sum_n et_{n,t}^o = es_t + eu_t + \sum_n et_{n,t}^i \tag{3}$$

In the bi-level optimization here, it is assumed that the lower level prosumers can only purchase energy from or sell energy via local energy transaction market at internal prices, and the upper level agent will transact with the external grid for supplement. Hence, for the upper level, the total energy balance (energy transaction with external grid, power charged to/discharged from GLIDES, energy transaction with lower level prosumer) is maintained in Eq.(3).

TABLE 1: Notation table for the upper level market operator

Index	
T, t	Decision periods, index for hours
Parameters	
Pp_t, Ps_t	Purchasing, selling price in power grid
$SV, \Delta t$	Size of pressure vessel, time period length
V_0, P_0	Initial volume and gas pressure in vessel
$\overline{V}, \underline{V}$	Max, min liquid volume in pressure vessel
$\overline{P}, \underline{P}$	Max, min pressure level in pressure vessel
η_P, η_M	Pump efficiency, motor efficiency of GLIDES
η_T, η_G	Turbine efficiency, generator efficiency of GLIDES
$\overline{\alpha}_c, \underline{\alpha}_c$	Coef. of max, min charging flow rate
$\overline{\alpha}_d, \underline{\alpha}_d$	Coef. of max, min discharging flow rate
Variables	
pt_t^+, pt_t^-	Electricity buying, selling price in local market
ep_t, es_t	Electricity bought from, sold to power grid
eu_t, eg_t	Electricity charging to, discharging from GLIDES
xc_t, xd_t	Binary status of pumping/generating of GLIDES
vc_t, vd_t	Charging, discharging flow rate of GLIDES
v_t, p_t	Liquid volume level, pressure level in GLIDES

4) Volume control in GLIDES

$$xc_t + xd_t \le 1 \tag{4}$$

$$\underline{V} \le v_t \le \overline{V} \tag{5}$$

$$v_T = V_0 \tag{6}$$

$$v_1 = V_0 + (vc_1 - vd_1) \tag{7}$$

$$v_t - v_{t-1} = (vc_t - vd_t), \forall t \ge 2 \tag{8}$$

$$\overline{V} \cdot \underline{\alpha}_c \cdot \Delta t \cdot xc_t \le vc_t \le \overline{V} \cdot \overline{\alpha}_c \cdot \Delta t \cdot xc_t \tag{9}$$

$$\overline{V} \cdot \underline{\alpha}_d \cdot \Delta t \cdot xd_t \le vd_t \le \overline{V} \cdot \overline{\alpha}_d \cdot \Delta t \cdot xd_t \tag{10}$$

For GLIDES energy storage, its liquid volume level in the pressure vessel should be kept between a permitted lowest level (Eq.(5)) and a maximum level, which is determined by the charging/discharging activities (Eq.(7)-(8)). The volumetric flow rate

TABLE 2: Notation table for the lower level prosumers

Index	
n,k	Index for buildings, segments in linearization
Parameters	
SP_n, SB_n	Size of solar panel, battery in buildings
$EB_{n,0}, \Delta t$	Initial energy level in battery, time period length
$El_{n,t}, Sol_t$	Nominal demand of buildings, solar radiation level
$\underline{El}_{n,t}, \overline{El}_{n,t}$	Lower bound, upper bound of power demand
$a_{n,t,k}, b_{n,t,k}$	Coef. of linear function for each segment
η_c, η_d	Charging, discharging efficiency of battery
$\underline{\alpha}_B, \overline{\alpha}_B$	Min, max coefficient of battery storage level
$\overline{\alpha}_c, \overline{\alpha}_d$	Max coefficient of charging, discharging of battery
γ, δ, ρ	Coef. of degradation, load shifting, load curtailment
Variables	
$el_{n,t}, lc_{n,t}$	Actual demand, inconvenience cost of load shifting
$et^i_{n,t}, et^o_{n,t}$	Electricity bought from, sold to local market
$ev_{n,t}, eb_{n,t}$	Electricity generation from PV, energy level in battery
$ec_{n,t}, ed_{n,t}$	Electricity charging to, discharging from battery

in the charging/discharging process cannot excess the range of the lowest and highest levels (Eq.(9)-(10)). Eq.(4)) ensures mutual exclusive charging/discharging status and Eq.(6)) ensures that the final liquid volume level at the end time period T should restore to its initial level.

5) Power generation for GLIDES

$$p_t/P_0 = [(SV - V_0)/(SV - v_t)]^u \tag{11}$$
$$eu_t \cdot \eta_P \cdot \eta_M \le vc_t \cdot p_t/3600 \tag{12}$$
$$eg_t \le \eta_T \cdot \eta_G \cdot vd_t \cdot p_t/3600 \tag{13}$$

The pressure-volume relation in Eq.(11) is given from the polytropic gas compression/expansion process between a min and max pressure Pascal. The polytropic index, u, is set to be 1.2 based on experimental data from the first lab-scale proof-of-concept GLIDES prototype in Oak Ridge National Laboratory. For the linearization of the bilinear terms in Eq.(12)-(13) and polytropic nonlinear term in Eq.(11), binary piecewise McCormick relaxation method is used, the reader could refer to our previous study [4].

3.2 Lower level model

1) Objective function for buildings

$$\begin{aligned}\min OC_n &= \textstyle\sum_t [(pt^+_t \cdot et^i_{n,t} - pt^-_t \cdot et^o_{n,t}) \\ &\quad + \delta \cdot (el_{n,t} - EL_{n,t})^2 + \gamma \cdot (ec_{n,t} + ed_{n,t})] \\ &= \textstyle\sum_t [(pt^+_t \cdot et^i_{n,t} - pt^-_t \cdot et^o_{n,t}) \\ &\quad + lc_{n,t} + \gamma \cdot (ec_{n,t} + ed_{n,t})]\end{aligned} \tag{14}$$

For each individual prosumer n, the objective is to minimize its operational cost OC_n, which equals the summation of the transaction cost in the internal market, inconvenience cost of load shifting, and the battery degradation cost. The quadratic term for the inconvenience cost could be linearized using piecewise segment method in ref [22] and substituted by $lc_{n,t}$ (Eq.(15)). For every constraint (numbered by c1, c2, etc.) in lower level model, its corresponding dual variable λ is also shown after the colons.

2) Load shifting linearization (c1)

$$a_{n,t,k} \cdot el_{n,t} + b_{n,t,k} \le lc_{n,t} : \lambda^{c1}_{n,t,k} \tag{15}$$

3) Electricity load balance (c2-c4)

$$ev_{n,t} + ed^d_{n,t} \cdot \eta_d + et^i_{n,t} = el_{n,t} + \frac{ec_{n,t}}{\eta_c} + et^o_{n,t} : \lambda^{c2}_{n,t} \tag{16}$$
$$\underline{El}_{n,t} \le el_{n,t} \le \overline{El}_{n,t} : \underline{\lambda}^{c3}_{n,t}, \overline{\lambda}^{c3}_{n,t} \tag{17}$$
$$\textstyle\sum_t el_{n,t} = (1-\rho) \cdot \sum_t El_{n,t} : \lambda^{c4}_n \tag{18}$$

The load balance for the lower level prosumer in Eq.(16) considers the energy generation from solar PV panel, battery discharging, and energy purchasing from local market on the left side, also the actual demand, battery charging, and energy sold to local market on the right side. Eq.(17) ensures that energy consumption should not drop below base load or exceed upper limit, and Eq.(18) ensures total usage for normal operation with potential curtailment.

4) PV generation (c5)

$$0 \le ev_{n,t} \le SP_n \cdot Sol_t \cdot \delta_V : \underline{\lambda}^{c5}_{n,t}, \overline{\lambda}^{c5}_{n,t} \tag{19}$$

The energy generation from solar PV panel could be estimated by its panel area, solar radiation level, and generation efficiency.

5) Battery storage (c6-c10)

$$0 \le ec_{n,t} \le SB_n \cdot \overline{\alpha}_c : \underline{\lambda}^{c6}_{n,t}, \overline{\lambda}^{c6}_{n,t} \tag{20}$$
$$0 \le ed_{n,t} \le SB_n \cdot \overline{\alpha}_d : \underline{\lambda}^{c7}_{n,t}, \overline{\lambda}^{c7}_{n,t} \tag{21}$$
$$eb_{n,T} = EB_{n,0} : \lambda^{c8}_n \tag{22}$$
$$SB_n \cdot \underline{\alpha}_B \le eb_{n,t} \le SB_n \cdot \overline{\alpha}_B : \underline{\lambda}^{c9}_{n,t}, \overline{\lambda}^{c9}_{n,t} \tag{23}$$
$$eb_{n,1} = EB_{n,0} + (ec_{n,1} - ed_{n,1}) \cdot \Delta t : \lambda^{c10}_{n,1} \tag{24}$$
$$eb_{n,t} - eb_{n,t-1} = (ec_{n,t} - ed_{n,t}) \cdot \Delta t : \lambda^{c10}_{n,t},\ \forall t \ge 2 \tag{25}$$

The relationship between charging/discharging power, available energy level and charging/discharging activities for battery storage could be modeled by Eq.(20)-(25), similarly as GLIDES energy storage.

6) Boundary constraints (c11-c12)

$$0 \le et^{i}_{n,t} : \lambda^{c11}_{n,t} \tag{26}$$

$$0 \le et^{o}_{n,t} : \lambda^{c12}_{n,t} \tag{27}$$

All the variables in the upper level and lower level model are positive. Here, the two variables for local energy transaction are explicitly defined as positive by Eq.(26)-(27) since they are not dependent on any other constraints above.

3.3 KKT transformation

To transform the bi-level optimization problem into a single-level optimization problem, the lower level problem can be replaced with its Karush-Kuhn-Tucker (KKT) conditions as the lower level model is continuous and linear and thus is convex. The Lagrangian function for the lower level model is assumed as L. It should be noted that the upper level variables pt_t^+ and pt_t^- should be treated as parameters for the lower level model. The KKT necessary conditions includes primal feasibility constraints, stationary constraints, complementary slackness constraints, dual feasibility constraints, shown as follows, respectively. For the continuous convex model here, these KKT necessary optimality conditions are also sufficient for optimality. More details on KKT based bi-level transformation could refer to [29].

1) Stationary Constraints

$$\frac{\partial L}{\partial el_{n,t}} = \sum_k (a_{n,t,k} \cdot \lambda^{c1}_{n,t,k}) + \lambda^{c2}_{n,t} - \underline{\lambda}^{c3}_{n,t} + \overline{\lambda}^{c3}_{n,t} - \lambda^{c4}_{n} = 0 \tag{28}$$

$$\frac{\partial L}{\partial lc_{n,t}} = 1 - \sum_k \lambda^{c1}_{n,t,k} = 0 \tag{29}$$

$$\frac{\partial L}{\partial ev_{n,t}} = -\lambda^{c2}_{n,t} - \underline{\lambda}^{c5}_{n,t} + \overline{\lambda}^{c5}_{n,t} = 0 \tag{30}$$

$$\frac{\partial L}{\partial ec_{n,t}} = \gamma + \frac{\lambda^{c2}_{n,t}}{\eta_c} - \underline{\lambda}^{c6}_{n,t} + \overline{\lambda}^{c6}_{n,t} + \lambda^{c10}_{n,t} = 0 \tag{31}$$

$$\frac{\partial L}{\partial ed_{n,t}} = \gamma - \lambda^{c2}_{n,t} \cdot \eta_d - \underline{\lambda}^{c7}_{n,t} + \overline{\lambda}^{c7}_{n,t} - \lambda^{c10}_{n,t} = 0 \tag{32}$$

$$\frac{\partial L}{\partial eb_{n,t\neq T}} = -\underline{\lambda}^{c9}_{n,t} + \overline{\lambda}^{c9}_{n,t} - \lambda^{c10}_{n,t} + \lambda^{c10}_{n,t+1} = 0 \tag{33}$$

$$\frac{\partial L}{\partial eb_{n,t=T}} = -\underline{\lambda}^{c9}_{n,t} + \overline{\lambda}^{c9}_{n,t} - \lambda^{c10}_{n,t} - \lambda^{c8}_{n} = 0 \tag{34}$$

$$\frac{\partial L}{\partial et^{i}_{n,t}} = pt^{+}_{t} - \lambda^{c2}_{n,t} - \lambda^{c11}_{n,t} = 0 \tag{35}$$

$$\frac{\partial L}{\partial et^{o}_{n,t}} = -pt^{-}_{t} + \lambda^{c2}_{n,t} - \lambda^{c12}_{n,t} = 0 \tag{36}$$

2) Complementary Slackness Constraints

$$0 \le (lc_{n,t} - a_{n,t,k} \cdot el_{n,t} - b_{n,t,k}) \perp \underline{\lambda}^{c1}_{n,t,k} \ge 0 \tag{37}$$

$$0 \le (el_{n,t} - \underline{El}_{n,t}) \perp \underline{\lambda}^{c3}_{n,t} \ge 0 \tag{38}$$

$$0 \le (\overline{El}_{n,t} - el_{n,t}) \perp \overline{\lambda}^{c3}_{n,t} \ge 0 \tag{39}$$

$$0 \le ev_{n,t} \perp \underline{\lambda}^{c5}_{n,t} \ge 0 \tag{40}$$

$$0 \le (SP_n \cdot Sol_t \cdot \delta_V - ev_{n,t}) \perp \overline{\lambda}^{c5}_{n,t} \ge 0 \tag{41}$$

$$0 \le ec_{n,t} \perp \underline{\lambda}^{c6}_{n,t} \ge 0 \tag{42}$$

$$0 \le (SB_n \cdot \overline{\alpha}_c - ec_{n,t}) \perp \overline{\lambda}^{c6}_{n,t} \ge 0 \tag{43}$$

$$0 \le ed_{n,t} \perp \underline{\lambda}^{c7}_{n,t} \ge 0 \tag{44}$$

$$0 \le (SB_n \cdot \overline{\alpha}_d - ed_{n,t}) \perp \overline{\lambda}^{c7}_{n,t} \ge 0 \tag{45}$$

$$0 \le (eb_{n,t} - SB_n \cdot \underline{\alpha}_B) \perp \underline{\lambda}^{c9}_{n,t} \ge 0 \tag{46}$$

$$0 \le (SB_n \cdot \overline{\alpha}_B - eb_{n,t}) \perp \overline{\lambda}^{c9}_{n,t} \ge 0 \tag{47}$$

$$0 \le et^{i}_{n,t} \perp \lambda^{c11}_{n,t} \ge 0 \tag{48}$$

$$0 \le et^{o}_{n,t} \perp \lambda^{c12}_{n,t} \ge 0 \tag{49}$$

As the constraints in Eq.(37) - (49) are nonlinear, auxiliary binary variables are introduced to recast each of these constraints into two linear constraints, for example, the constraint Eq.(37) could be written as:

$$lc_{n,t} - a_{n,t,k} \cdot el_{n,t} - b_{n,t,k} \le M \cdot \underline{x}^{c1}_{n,t,k} \tag{50}$$

$$\underline{\lambda}^{c1}_{n,t,k} \le M \cdot (1 - \underline{x}^{c1}_{n,t,k}) \tag{51}$$

where $\underline{x}^{c1}_{n,t,k}$ is binary variable and M is sufficiently large positive constant.

3) Dual feasibility

Dual variables are free variables if the primal constraints are equations, and all other dual variables should be nonnegative, see the following constraints

$$\lambda^{c2}_{n,t}, \lambda^{c4}_{n}, \lambda^{c8}_{n}, \lambda^{c10}_{n,t} \in \mathbb{R} \tag{52}$$

$$\lambda^{c1}_{n,t}, \underline{\lambda}^{c3}_{n,t}, \overline{\lambda}^{c3}_{n,t}, \underline{\lambda}^{c5}_{n,t}, \overline{\lambda}^{c5}_{n,t}, \underline{\lambda}^{c6}_{n,t}, \overline{\lambda}^{c6}_{n,t} \ge 0 \tag{53}$$

$$\underline{\lambda}^{c7}_{n,t}, \overline{\lambda}^{c7}_{n,t}, \underline{\lambda}^{c9}_{n,t}, \overline{\lambda}^{c9}_{n,t}, \lambda^{c11}_{n,t}, \lambda^{c12}_{n,t} \ge 0 \tag{54}$$

4) Strong duality property

According to the strong duality theory, the objective of the primal problem is equal to the objective of the corresponding dual problem, therefore, the lower level objective function Eq.(14) satisfies the following relationship when the lower level

problem reaches optimality.

$$\begin{aligned}
&\textstyle\sum_t \left[(pt_t^+ \cdot et_{n,t}^i - pt_t^- \cdot et_{n,t}^o) + lc_{n,t} + \gamma \cdot (ec_{n,t} + ed_{n,t})\right] \\
&= \textstyle\sum_t \Big[\sum_k (\lambda_{n,t,k}^{c1} \cdot b_{n,t,k}) + \underline{\lambda}_{n,t}^{c3} \cdot \underline{El}_{n,t} - \overline{\lambda}_{n,t}^{c3} \cdot \overline{El}_{n,t} \\
&\quad + \lambda_n^{c4} \cdot (1-\rho) \cdot El_{n,t} - \overline{\lambda}_{n,t}^{c5} \cdot SP_n \cdot Sol_t \cdot \delta_V \\
&\quad - \overline{\lambda}_{n,t}^{c6} \cdot SB_n \cdot \overline{\alpha}_c - \overline{\lambda}_{n,t}^{c7} \cdot SB_n \cdot \overline{\alpha}_d + \underline{\lambda}_{n,t}^{c9} \cdot SB_n \cdot \underline{\alpha}_B \\
&\quad - \overline{\lambda}_{n,t}^{c9} \cdot SB_n \cdot \overline{\alpha}_B\Big] + \lambda_n^{c8} \cdot EB_{n,0} + \lambda_{n,1}^{c10} \cdot EB_{n,0}
\end{aligned} \tag{55}$$

Due to equation (55), the bilinear term $\sum_{n,t}(pt_t^+ \cdot et_{n,t}^i - pt_t^- \cdot et_{n,t}^o)$ in the upper level objective function Eq.(1) could be substituted. The resulted single level optimization model is a mixed-integer linear program as follows. It could be solved to global optimal by off-the-shelf solvers, like CPLEX, GUROBI.

$$\begin{aligned}
\max OR = &\textstyle\sum_t (Ps_t \cdot es_t - Pp_t \cdot ep_t) \\
&+ \textstyle\sum_n \Big\{\sum_t \Big[\sum_k (\lambda_{n,t,k}^{c1} \cdot b_{n,t,k}) + \underline{\lambda}_{n,t}^{c3} \cdot \underline{El}_{n,t} \\
&- \overline{\lambda}_{n,t}^{c3} \cdot \overline{El}_{n,t} + \lambda_n^{c4} \cdot (1-\rho) \cdot El_{n,t} \\
&- \overline{\lambda}_{n,t}^{c5} \cdot SP_n \cdot Sol_t \cdot \delta_V - \overline{\lambda}_{n,t}^{c6} \cdot SB_n \cdot \overline{\alpha}_c \\
&- \overline{\lambda}_{n,t}^{c7} \cdot SB_n \cdot \overline{\alpha}_d + \underline{\lambda}_{n,t}^{c9} \cdot SB_n \cdot \underline{\alpha}_B \\
&- \overline{\lambda}_{n,t}^{c9} \cdot SB_n \cdot \overline{\alpha}_B\Big] + \lambda_n^{c8} \cdot EB_{n,0} + \lambda_{n,1}^{c10} \cdot EB_{n,0}\Big\} \\
&- \textstyle\sum_n \sum_t \left[lc_{n,t} + \gamma \cdot (ec_{n,t} + ed_{n,t})\right]
\end{aligned} \tag{56}$$

And the final constraint sets for the resulted single level optimization includes: upper level constraints (2)-(13), lower level primal feasibility constraints (15)-(27), lower level stationary constraints (28)-(36), linearized version for lower level complementary slackness constraints (37)-(49), and lower level dual feasibility constraints (52)-(54)

4 Numerical Experiments

For the GLIDES system in the upper level, one pressure vessel with 20 kW rated power and 4 hours of storage time is assumed here. The other parameter settings of GLIDES are listed in Table 3.

TABLE 3: Parameter settings for the GLIDES system

Parameter	$\overline{P}$(kpa)	$\underline{P}$	$\overline{V}(m^3)$	$\underline{V}$	SV	V_0	P_0
Value	13000	7000	37.211	0	92.331	18.605	9170.095
Parameter	η_P, η_M	η_T, η_G	$\overline{\alpha}_c, \overline{\alpha}_d$	$\underline{\alpha}_c, \underline{\alpha}_d$	–	–	–
Value	0.9,0.9	0.9,0.9	0.25	0.083	–	–	–

Three prosumers: large office $n1$, supermarket $n2$, and large hotel $n3$ are assumed for the lower level in this research. Their nominal load profile El are obtained from the reference data for commercial buildings maintained by the U.S. Department of Energy [30] and scaled to the same level. By name order, PV size and power capacity of battery are set as $SP = [180, 200, 200](m^2)$, $SB = [150, 100, 120](kW)$. The following parameters are set to be same for all prosumers: $\eta_V = 0.25$, $\underline{\alpha}_b = 0.05$, $\overline{\alpha}_b = 1$, $\overline{\alpha}_c = 0.25$, $\overline{\alpha}_d = 0.1$, $\eta_c = \eta_d = 0.95$, $\gamma = 0.008$, $\rho = 0$. For each hour, $\underline{El} = 0.8 \cdot El$, $\overline{El} = 1.2 \cdot El$. Initial energy level $EB = 0.5 \cdot SB$. The nominal load profile and net load profile (equals nominal load - solar power) for prosumers $n1 \sim n3$ are shown in Figure 5-6. Since the available solar power mainly concentrates in the time period 6:00 to 20:00, hence, this time period is chosen as the decision period (totally 15 hours) in this research.

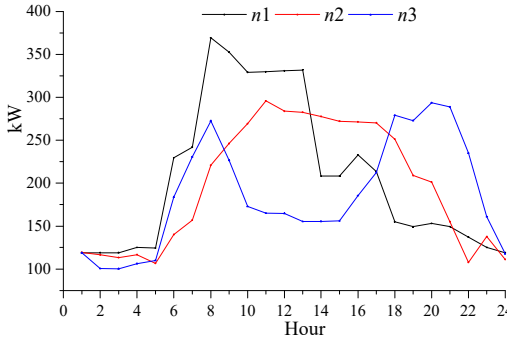

FIGURE 5: Nominal demand of three prosumers

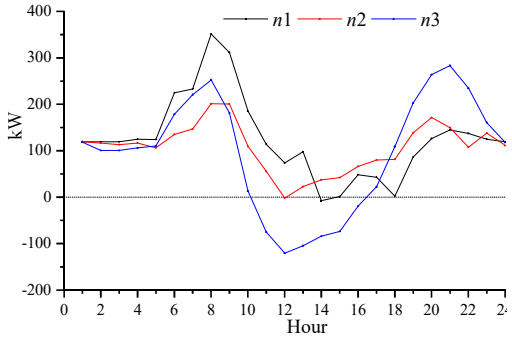

FIGURE 6: Net demand of three prosumers

To study energy transaction in local market, two different transaction price structures (equal $pt^+ = pt^-$) and (nonequal $pt^+ \geq pt^-$) and three different demand response level ($\delta = 0.001, 0.005, 0.01$) for prosumers are compared in the experiments. The obtained transaction prices are shown in Figure 7-9.

External prices (dash lines) are the upper and lower bound for local market and the transaction prices from equal price structure (blue line) are always within the range of local buying (black line) and selling prices (red line) for the nonequal price structure.

Since the upper level agent is trying to maximize its profit, it intends to set the local transaction prices as close as the external prices, for instance, the upper level has set the local buying price pt^+ to be the external buying price Pp before 10:00 and after 17:00 as the net demand profile indicates that there won't be surplus energy for transaction in these two time periods (load shifting needs to be considered). Meantime, when there are potential local transaction, the upper level also needs to take the responses from all lower level prosumers into account when setting the best prices because the prices will affect their local energy transaction amount.

The liquid volume level in the pressure vessel of GLIDES is also plotted in Figure 10 for $\delta = 0.001$ case. The discharged power of GLIDES with equal price structure is less than that of nonequal price structure, which implies more local energy transaction among prosumers with equal price structure. This conclusion could be backed up by the local energy transaction amount results shown in Figure 11-12, which shows prosumer $n3$ sold more energy and $n1, n2$ have bought more energy (between 10:00 and 17:00) when local buying and selling prices are set to be equal.

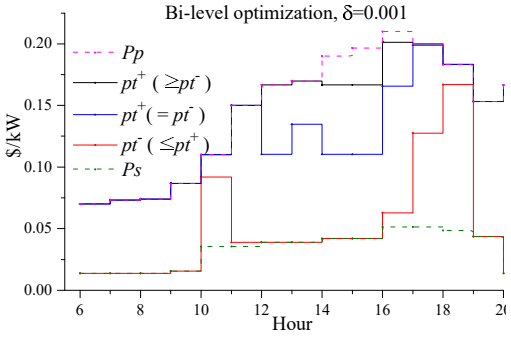

FIGURE 7: Local energy transaction price ($\delta = 0.001$)

In order to compare the cost and benefit distribution in the bi-level optimization, single level separate operation for the three prosumers are also conducted. In the separate operation, local energy transaction is not allowed and each prosumer optimizes its own operation schedule based on external prices Pp, Ps. All the detailed results are summarized into Table 4.

In the separate operation, GLIDES has zero profit because external grid Pp is greater than Ps all the time and thus there is no arbitrage space. For individual prosumers, their cost will be slightly lower if they are less sensitive to load shifting (lower

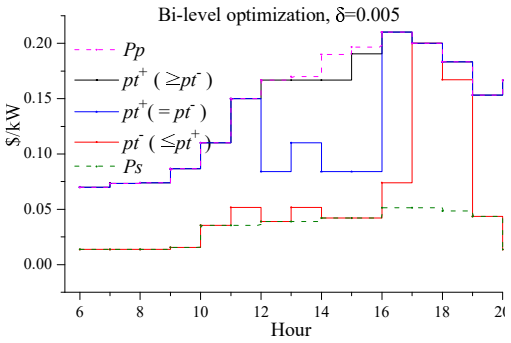

FIGURE 8: Local energy transaction price ($\delta = 0.005$)

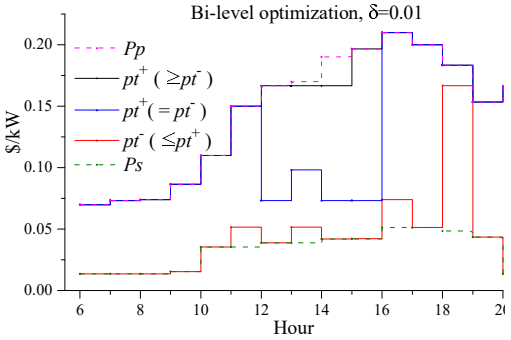

FIGURE 9: Local energy transaction price ($\delta = 0.01$)

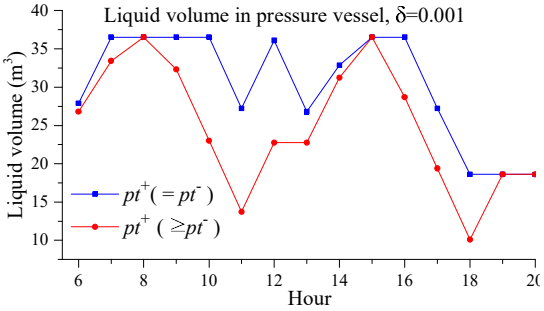

FIGURE 10: Liquid volume in pressure vessel ($\delta = 0.001$)

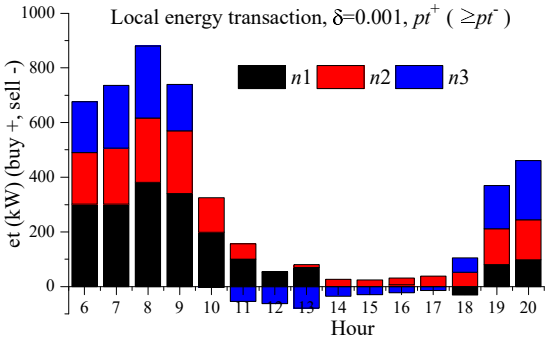

FIGURE 11: Local energy transaction ($pt^+ \geq pt^-$)

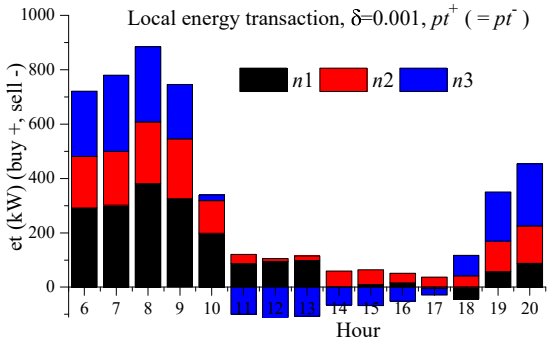

FIGURE 12: Local energy transaction ($pt^+ = pt^-$)

δ) for both separate operation and bi-level optimization. When the local market adopts equal price structure, as mentioned, more local energy transaction is expected (comparison between Figure 11 and 12) and each prosumer could share more benefit due to lower local prices, however, the upper level GLIDES will have less revenue potential with equal transaction price, around $\$2 \sim 3$ in Table 4. When local transaction prices are not equal, the upper level has more arbitrage space to boost its revenue from around \$3 to \$45, meanwhile, the prosumers' cost increases as compared to equal price structure but it is still guaranteed (by lower local transaction prices) to be not greater than the cost in the separate operation.

TABLE 4: Cost comparison for the bi-level optimization with different internal price structures

Separate	Profit (\$)	Operation Cost (\$)		
Pp, Ps	GLIDES	$n1$	$n2$	$n3$
$\delta = 0.001$	0	191.621	173.417	129.127
$\delta = 0.005$	0	197.835	181.052	136.526
$\delta = 0.01$	0	198.595	181.997	138.288
Bi-level	Profit (\$)	Operation Cost (\$)		
$pt^+ = pt^-$	GLIDES	$n1$	$n2$	$n3$
$\delta = 0.001$	2.237	183.466	166.532	94.222
$\delta = 0.005$	3.072	185.361	171.337	107.426
$\delta = 0.01$	3.282	184.113	170.892	112.371
$pt^+ \geq pt^-$	GLIDES	$n1$	$n2$	$n3$
$\delta = 0.001$	37.767	191.357	172.492	128.899
$\delta = 0.005$	45.055	197.503	180.172	134.212
$\delta = 0.01$	46.405	198.267	181.267	135.724

CONCLUSION

In this work, an application case of local energy trading in smart community is studied for a novel modular pump hydro storage. Bi-level optimization is adopted for energy pricing and trading locally with GLIDES as the upper level agent and three commercial buildings as the lower level prosumers. Detailed KKT conditions for the lower level model is derived to transform bi-level optimization into single level mixed-integer linear optimization. With lower energy transaction prices, prosumers are promoted to be involved in the local market and their operation cost will be guaranteed to be lower than the separate operation. The results also indicate revenue potential for the upper level agent is between $\$2 \sim \$45$ depending on the local price structure in studied cases. More cooperative optimization and profit sharing in the local market will be studied in the future.

ACKNOWLEDGMENT

This work was funded by the Department of Energy, Energy Efficiency and Renewable Energy Office under the Building Technologies Program.

REFERENCES

[1] REN21, 2019. Renewables 2019 global status report. Tech. rep.

[2] U.S. Energy Information Administration, 2020. Annual Energy Outlook 2020 (with projections to 2050). Tech. rep.

[3] Balducci, P. J., Alam, M. J. E., Hardy, T. D., and Wu, D., 2018. "Assigning value to energy storage systems at multiple points in an electrical grid". *Energy Environ. Sci.,* ***11***, pp. 1926–1944.

[4] Chen, Y., Odukomaiya, A., Kassaee, S., O'Connor, P., Momen, A. M., Liu, X., and Smith, B. T., 2019. "Preliminary analysis of market potential for a hydropneumatic ground-level integrated diverse energy storage system". *Applied Energy,* ***242***, pp. 1237 – 1247.

[5] Center for Sustainable Systems, University of Michigan, 2019. U.S. Grid Energy Storage Factsheet. Tech. Rep. Pub.No. CSS15-17.

[6] National Hydropower Association (NHA), 2012. "Challenges and Opportunities for New Pumped Storage Development".

[7] Whittingham, M. S., 2012. "History, evolution, and future status of energy storage". *Proceedings of the IEEE,* ***100***(Special Centennial Issue), May, pp. 1518–1534.

[8] Chen, Y., Dababneh, F., Zhang, B., Kassaee, S., Smith, B. T., Liu, X., and Momen, A. M., 2019. "Surrogate Modeling for Capacity Planning of Charging Station Equipped With Photovoltaic Panel and Hydropneumatic Energy Storage". *Journal of Energy Resources Technology,* ***142***(5), 01. 050907.

[9] Gkatzikis, L., Koutsopoulos, I., and Salonidis, T., 2013. "The role of aggregators in smart grid demand response markets". *IEEE Journal on Selected Areas in Communications,* ***31***(7), July, pp. 1247–1257.

[10] Tang, Y., Chen, Q., Ning, J., Wang, Q., Feng, S., and Li, Y., 2018. "Hierarchical control strategy for residential demand response considering time-varying aggregated capacity". *International Journal of Electrical Power & Energy Systems,* ***97***, pp. 165 – 173.

[11] Yang, P., Tang, G., and Nehorai, A., 2013. "A game-theoretic approach for optimal time-of-use electricity pricing". *IEEE Transactions on Power Systems,* ***28***(2), May, pp. 884–892.

[12] Yu, M., and Hong, S. H., 2016. "Supply–demand balancing for power management in smart grid: A stackelberg game approach". *Applied Energy,* ***164***, pp. 702 – 710.

[13] Belgana, A., Rimal, B. P., and Maier, M., 2015. "Open energy market strategies in microgrids: A stackelberg game approach based on a hybrid multiobjective evolutionary algorithm". *IEEE Transactions on Smart Grid,* ***6***(3), May, pp. 1243–1252.

[14] Xu, Z., Deng, T., Hu, Z., Song, Y., and Wang, J., 2018. "Data-driven pricing strategy for demand-side resource aggregators". *IEEE Transactions on Smart Grid,* ***9***(1), Jan, pp. 57–66.

[15] Bremdal, B. A., Olivella-Rosell, P., Rajasekharan, J., and Ilieva, I., 2017. "Creating a local energy market". *CIRED - Open Access Proceedings Journal,* ***2017***(1), pp. 2649–2652.

[16] Chen, Y., and Hu, M., 2016. "Balancing collective and individual interests in transactive energy management of interconnected micro-grid clusters". *Energy,* ***109***, pp. 1075 – 1085.

[17] Zhang, C., Wu, J., Zhou, Y., Cheng, M., and Long, C., 2018. "Peer-to-peer energy trading in a microgrid". *Applied Energy,* ***220***, pp. 1 – 12.

[18] Chen, Y., and Hu, M., 2018. "A swarm intelligence based distributed decision approach for transactive operation of networked building clusters". *Energy and Buildings,* ***169***, pp. 172 – 184.

[19] Chen, Y., and Hu, M., 2019. "Swarm intelligence–based distributed stochastic model predictive control for transactive operation of networked building clusters". *Energy and Buildings,* ***198***, pp. 207 – 215.

[20] Zugno, M., Morales, J. M., Pinson, P., and Madsen, H., 2013. "A bilevel model for electricity retailers' participation in a demand response market environment". *Energy Economics,* ***36***, pp. 182 – 197.

[21] Bahramara, S., Moghaddam, M. P., and Haghifam, M., 2016. "A bi-level optimization model for operation of distribution networks with micro-grids". *International Journal of Electrical Power & Energy Systems,* ***82***, pp. 169 – 178.

[22] Cui, S., Wang, Y., Xiao, J., and Liu, N., 2019. "A two-stage robust energy sharing management for prosumer microgrid". *IEEE Transactions on Industrial Informatics,* ***15***(5), May, pp. 2741–2752.

[23] Momen, A. M., Gluesenkamp, K. J., Abdelaziz, O. A., Vineyard, E. A., Abu-heiba, A., and Odukomaiya, A. O., 2017. "Near Isothermal Combined Compressed Gas/Pumped-Hydro Electricity Storage with Waste Heat Recovery Capabilities". *U.S. Patent No. 10519923*, pp. Issued: December 31, 2019.

[24] Odukomaiya, A., Abu-Heiba, A., Gluesenkamp, K. R., Abdelaziz, O., Jackson, R. K., Daniel, C., Graham, S., and Momen, A. M., 2016. "Thermal analysis of near-isothermal compressed gas energy storage system". *Applied Energy,* ***179***, pp. 948–960.

[25] Odukomaiya, A., Abu-Heiba, A., Graham, S., and Momen, A. M., 2018. "Experimental and analytical evaluation of a hydro-pneumatic compressed-air Ground-Level Integrated Diverse Energy Storage (GLIDES) system". *Applied Energy,* ***221***(April), pp. 75–85.

[26] Sciacovelli, A., Smith, D., Navarro, M. E., Vecchi, A., Peng, X., Li, Y., Radcliffe, J., and Ding, Y., 2017. "Performance Analysis and Detailed Experimental Results of the First Liquid Air Energy Storage Plant in the World". *Journal of Energy Resources Technology,* ***140***(2), 11.

[27] McTigue, J. D., White, A. J., and Markides, C. N., 2015. "Parametric studies and optimisation of pumped thermal electricity storage". *Applied Energy,* ***137***, pp. 800 – 811.

[28] Kassaee, S., Abu-Heiba, A., Ally, M. R., Mench, M. M., Liu, X., Odukomaiya, A., Chen, Y., King, T. J., Smith, B. T., and Momen, A. M., 2019. "Part 1- techno-economic analysis of a grid scale ground-level integrated diverse energy storage (glides) technology". *Journal of Energy Storage,* ***25***, p. 100792.

[29] Dempe, S., and Franke, S., 2019. "Solution of bilevel optimization problems using the kkt approach". *Optimization,* ***68***(8), pp. 1471–1489.

[30] U.S. Department of Energy, 2020. Commercial reference buildings, https://www.energy.gov/eere/buildings/commercial-reference-buildings.